

Analysis of DC/DC converters by mean node voltage method

G. Vitale

National Research Council of Italy, CNR – ISSIA UOS Palermo,
 Via Dante n. 12, 90141 Palermo, email: vitale (at) pa.issia.cnr.it

Abstract. This paper proposes the analysis of buck, boost and buck-boost converters by the mean node voltage method to implement them in simulink® environment. The corresponding equivalent linear circuit in the s-domain are determined and the static gain, the audio susceptibility function, the output impedance and the control-to-output transfer functions are deduced accounting for the parasitic effects of inductors and capacitors as well. This approach is simpler compared to the state space averaging method and allows the simulation time to be reduced. The implementation in Simulink environment® of the converters are described and finally the simulated waveforms of a buck converter are compared with the experimental ones.

Key words

DC/DC converter, buck, boost, buck-boost, simulink® implementation, renewable energy systems.

1. Introduction

Switching DC/DC converters in the last years, have increased the interest on power conversion systems for distributed energy resources (DER) since the power is usually generated at DC voltage and many loads require power at constant DC voltage as well. Although the first studies on DC/DC converters date from about forty years ago, recently several books dealing with DC/DC converters analysis, design, control and their use in the field of Renewables have been published [1-5].

There are many applications of DC/DC converters in the field of Renewable Energy Sources (RES) where they are employed to interface the source with the inverter by tracking, at the same time, the Maximum Power Point [6-11]. In addition to vessels, aircrafts and other systems operated in islanding in which DC distribution is adopted, their use with a grid connection have been studied as well [12], this leads to simplify the distribution architecture with an increase of the efficiency [13]. In particular, the interest has been increased by the development of smart grids where an intelligent management of energy distribution allows energy distribution to be optimally exploited [14-16]. Finally by a controlled DC/DC converter an emulator of a RES or a Fuel Cell can be realized for laboratory research purposes [17-20]. The above cited applications justify further studies on the DC/DC converters modelling and control to define models that are simple to be implemented and require a low computation time as that proposed in this paper. This is particularly useful for the analysis of the whole power conversion chain in renewable energy systems (RES).

As it is known, basic topologies of switching DC/DC converters, as buck, boost and buck-boost, are

characterised by a unique switch. They are simple and offer a high efficiency. On the other hand, the correct operation must be achieved by feedback control. The dynamic behaviour is described by audio susceptibility function, the output impedance and by the control-to-output transfer function. They can be obtained by state space averaging approach, which requires the knowledge of the state space representation. In this paper the circuits are studied in the Laplace domain, the mean potential of the nodes are identified so that, both the static gain and the transfer functions can be obtained simply by the Kirchhoff's laws. This approach allows a Simulink® implementation to be easily performed without the use of specific circuit simulator and a reduction of the computation time.

2. Dynamic behaviour characterization

The dynamic behaviour refers to the output voltage variations. It can vary for: a) the variation of the input voltage, b) the variation of the current required by the load, c) the variation of the duty cycle. The case a) is described by the audio susceptibility function defined as the ratio of the small variations of the input voltage vs. the output voltage; the case b) is described by the output impedance defined as the ratio of the small variations of the output current vs. the output voltage and finally the case c) is described by the control-to-output transfer function defined by the ratio of the small variation of the output voltage vs. the duty cycle. This situation is represented in the block diagram of figure 1, where, to assure that the output voltage remains constant against the input variations, a feedback acting on the duty cycle is performed.

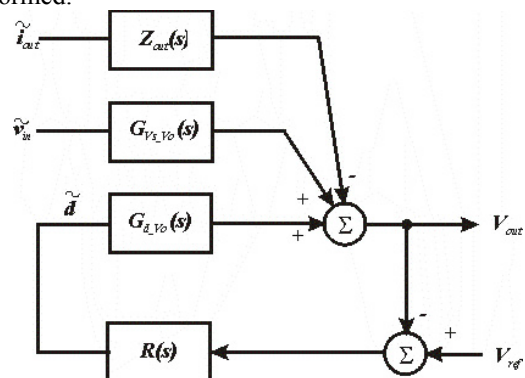


Fig. 1. Representation of the influence of the variations of the output current, of the input voltage and of the duty cycle on the output voltage of a DC/DC converter

It can be observed that the lower is the output impedance (the audio susceptibility function), the lower will be the output voltage variations for a variation of the output current (input voltage). The presence of the feedback modifies the transfer functions as shown below.

$$\begin{cases} G_{v_{ref_Vo}} = \frac{\tilde{v}_{out}}{\tilde{v}_{ref}} = \frac{L(s)}{1+L(s)} \\ G_{V_s_Vo}^{CL} = \frac{\tilde{v}_{out}}{\tilde{v}_{in}} = \frac{G_{V_s_Vo}(s)}{1+L(s)} \\ Z_{out}^{CL} = -\frac{\tilde{v}_{out}}{\tilde{i}_{out}} = \frac{Z_{out}(s)}{1+L(s)} \end{cases} \quad (1)$$

where:

$$L(s) = G_{d_vo}(s)R(s)$$

3. Analysis of the buck converter

The analysis of DC/DC converters by linear circuits are deeply explained in [21]; in this paper the fundamentals are recalled to explain the proposed implementation in simulink® environment in s-domain.

The buck converter topology is shown in figure 2. Four nodes are recognizable: the ground node, the input node whose voltage is forced by the input supply, the output node and an intermediate node which has a mean voltage given by the product of the input voltage for the duty cycle ($V_s \cdot D$). As a matter of fact the voltage of this intermediate node is given by:

$$V_{int} = (V_s \cdot t_{on} + 0 \cdot t_{off}) / T = V_s D \quad (2)$$

Where T is the switching period ($T=1/f$), t_{on} is the time interval in which the switch is in the ON state, t_{off} is the time interval in which the switch is in the OFF state ($t_{on}+t_{off}=T$) and D is the duty cycle defined as t_{on}/T . For this, the circuit can be redrawn by considering the equivalent supply $V_s \cdot D$ as sketched in figure 3.

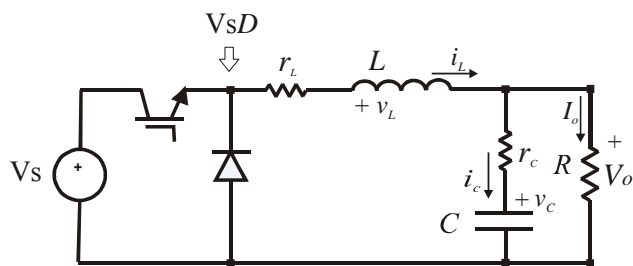


Fig. 2. Circuit of the Buck converter

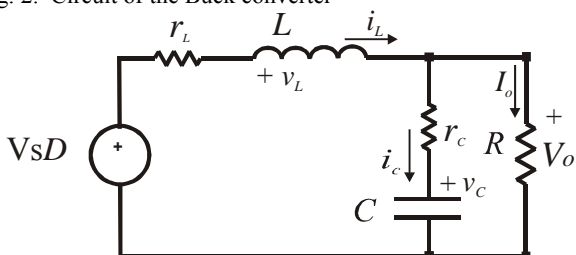


Fig. 3. Linear equivalent scheme of the Buck converter

The State space equations can be derived by the circuit of figure 3 using the Kirchhoff's voltage law (LKV) applied to the external loop and the Kirchhoff's current law (LKI) applied to the output node. By manipulating (3) and taking into account the approximation (4), the equations (5) are obtained.

$$\begin{cases} V_s D = i_L r_L + L \frac{di_L}{dt} + V_o \\ i_L = C \frac{dv_c}{dt} + \frac{V_o}{R} \end{cases} \quad (3)$$

$$V_o = r_c i_c + v_c \approx v_c \quad (4)$$

$$\begin{cases} \frac{di_L}{dt} = -\frac{r_L}{L} i_L - \frac{1}{L} v_c + \frac{1}{L} V_s D \\ \frac{dv_c}{dt} = \frac{1}{C} i_L - \frac{1}{CR} v_c \end{cases} \quad (5)$$

A. Static Gain evaluation

The static gain can be obtained considering the circuit of figure 4, it is the DC version respect to the circuit of figure 3. The static gain V_s / V_o is given by (6).

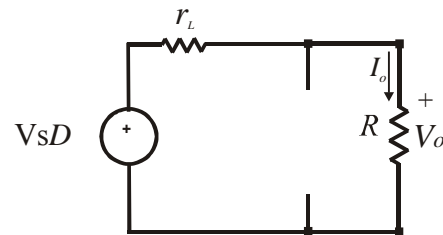


Fig. 4. Equivalent DC circuit of the buck converter

$$\frac{V_o}{V_s} = D \frac{R}{R + r_L} \quad (6)$$

B. Audio susceptibility function

With reference to the circuit of figure 2, and defining the quantities:

$$\begin{cases} Z_L = sL + r_L \\ Z_C = \frac{1}{sC} + r_c \end{cases} \quad (7)$$

The output voltage can be calculated considering that the input voltage is partitioned by Z_L and by the parallel formed by the impedance of the capacitor and the load ($Z_C // R$).

$$V_o(s) = D \cdot V_s(s) \frac{Z_C // R}{Z_L + (Z_C // R)} \quad (8)$$

The input voltage, the output voltage and the duty cycle contains a DC plus a AC quantity, hence indicating with “-” the DC components, with “~” the AC components

and neglecting the product of AC terms, the audio susceptibility function can be found by setting $\tilde{d} = 0$.

$$\bar{V}_0 + \tilde{v}_0(s) = (\bar{D} + \tilde{d})(\bar{V}_s + \tilde{v}_s(s)) \frac{Z_C // R}{Z_L + (Z_C // R)} \quad (9)$$

From which:

$$\frac{\tilde{v}_0(s)}{\tilde{v}_s(s)} = D \frac{(sCr_C + 1)R}{s^2RLC + s[L + RC(r_C + r_L)] + r_C + R} \quad (10)$$

Where, for the sake of readability, the DC value of the duty cycle is written as D instead of \bar{D} .

C. control-to-output transfer function

The control-to-output transfer function is easily obtained by (9) setting $\tilde{v}_s = 0$.

$$\frac{\tilde{v}_0(s)}{\tilde{d}(s)} = V_s \frac{(sCr_C + 1)R}{s^2RLC + s[L + RC(r_C + r_L)] + r_C + R} \quad (11)$$

D. Output impedance

The output impedance is calculated with reference to the circuit of figure 5 where $V_s=0$ and the output is supplied by a current generator equal to $-I_{out}$. It is given by the parallel of Z_L , Z_C and the load R .

$$Z_{out} = -\frac{\tilde{v}_0(s)}{\tilde{I}_{out}(s)} = \frac{R(sCr_C + 1)(sL + r_L)}{s^2LC(R + r_C) + s[L + RC(r_C + r_L) + (r_C r_L C)] + R + r_L} \quad (12)$$

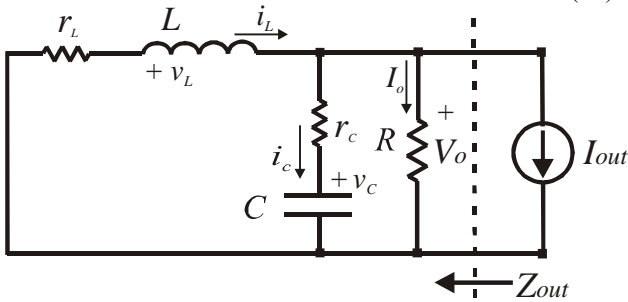


Fig. 5. Equivalent circuit of the buck converter for calculating Z_{out} .

4. Analysis of the boost converter

The circuit of the boost converter is shown in figure 6. The voltage of the intermediate node is equal to zero during T_{on} and equal to V_o during T_{off} . Hence, its mean voltage is given by $V_{int} = V_o(1-D)$. The current flowing through the diode is null during T_{ons} , as a consequence, it has a mean value given by $I_L(1-D)$. On the basis of these considerations, the equivalent scheme of figure 7 can be drawn. In this circuit there is a voltage dependent voltage source and a current dependent current source which reproduce the voltage at the intermediate node and the current flowing through the inductance respectively.

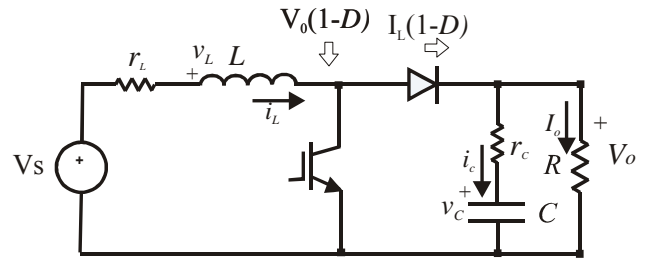


Fig. 6. Circuit of the Boost converter

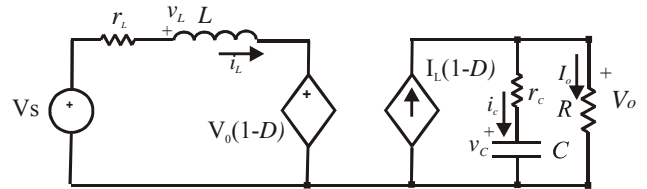


Fig. 7. Linear equivalent circuit of the Boost converter

The state space equations can be derived by the circuit of figure 7 by using the LKV applied to the input loop and the LKI to the output node. By manipulating (13) and taking into account the approximation (14), the state space equations (15) are obtained.

$$\begin{cases} V_s = i_L r_L + L \frac{di_L}{dt} + V_o(1-D) \\ i_L(1-D) = C \frac{dv_c}{dt} + \frac{V_o}{R} \end{cases} \quad (13)$$

$$V_o = r_C i_c + v_c \approx v_c \quad (14)$$

From which

$$\begin{cases} \frac{di_L}{dt} = -\frac{i_L r_L}{L} - \frac{v_c}{L}(1-D) + \frac{V_s}{L} \\ \frac{dv_c}{dt} = \frac{i_L}{C}(1-D) - \frac{v_c}{RC} \end{cases} \quad (15)$$

The well known bilinear form, in which a nonlinearity in the product of the state variables and the control variable occurs, is obtained.

A. Static Gain evaluation

The static gain can be obtained considering the circuit of figure 8, it is the DC version of the circuit of figure 7. The static gain V_s / V_o is obtained considering that the output voltage is given by the inductor current multiplied by the load R and that the inductor current is calculated by the difference of input voltage and the potential of the voltage dependent voltage source divided by r_L .

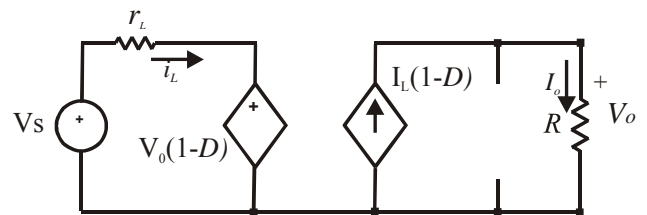


Fig. 8. Equivalent DC circuit of the boost converter

$$V_o = I_L(1-D)R = \frac{V_s - V_o(1-D)}{r_L}(1-D)R \quad (13)$$

From which:

$$\frac{V_o}{V_s} = \frac{R(1-D)}{R(1-D)^2 + r_L} \quad (14)$$

B. Audio susceptibility function

From the circuit of figure 7, by the LKI on the output node, the following equation can be written:

$$\frac{V_s - V_o(1-D)}{sL + r_L}(1-D) = \frac{V_o}{r_c + 1/sC} + \frac{V_o}{R} \quad (15)$$

From which:

$$V_o(s) = V_s(s) \frac{(sCr_c + 1)R(1-D)}{s^2RLC + s[L + RCr_L + (1-D)^2RCr_c] + R(1-D)^2 + r_L} \quad (16)$$

By writing the input voltage, the output voltage and the duty cycle as the sum of their DC and AC quantities, and taking into account that:

$$\begin{cases} (1-D) = 1 - \bar{D} - \tilde{d} \\ (1-D)^2 = (1 - \bar{D})^2 - 2(1 - \bar{D})\tilde{d} \end{cases} \quad (17)$$

the audio susceptibility function is calculated by setting $\tilde{d} = 0$.

$$\frac{\tilde{v}_o(s)}{\tilde{v}_s(s)} = \frac{(sCr_c + 1)R(1-D)}{s^2RLC + s[L + RCr_L + (1-D)^2RCr_c] + R(1-D)^2 + r_L} \quad (18)$$

C. Control-to-output transfer function

The control-to-output transfer function is obtained by (16) taking into account (17) and setting $\tilde{v}_s = 0$.

$$\frac{\tilde{v}_o(s)}{\tilde{d}(s)} = \frac{[-V_s + 2V_o(1-D)](sCr_c + 1)R}{s^2RLC + s[L + RCr_L + (1-D)^2RCr_c] + R(1-D)^2 + r_L} \quad (19)$$

D. Output impedance

The output impedance of the boost converter can be calculated by the circuit drawn in figure 9 where the supply V_s is set to zero. The LKI on the output node gives:

$$i_L(1-D) = \frac{V_o}{r_c + 1/sC} + \frac{V_o}{R} + I_{out} \quad (20)$$

by taking into account that

$$i_L = \frac{V_o(1-D)}{sL + r_L} \quad (21)$$

and substituting (20) into (21), after some manipulations, the following expression is obtained:

$$Z_{out} = -\frac{\tilde{I}_{out}(s)}{\tilde{v}_o(s)} = \frac{R(sCr_c + 1)(sL + r_L)}{s^2LC(R + r_c) + s[L + RCr_c(1-D)^2 + Cr_c(R + r_c)] + R(1-D)^2 + r_L} \quad (22)$$

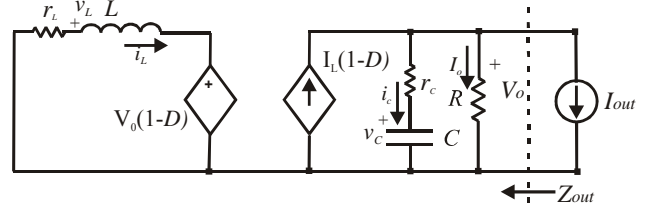


Fig. 9. Equivalent circuit of the boost converter for calculating Z_{out} .

5. Analysis of the buck-boost converter

The circuit of the buck-boost converter is sketched in figure 10. It can be noted that the positive of the voltage V_o is on the ground node.

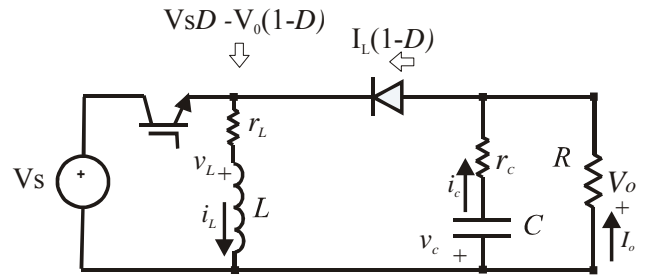


Fig. 10. Circuit of the buck-boost converter

The voltage of the intermediate node is equal to V_s during t_{on} and equal to V_o during t_{off} , hence its mean voltage is equal to:

$$V_{int} = [V_s \cdot t_{on} + V_o \cdot t_{off}] / T = V_s D - V_o(1-D) \quad (23)$$

The current flowing through the diode is equal to the current in the inductance during t_{off} and it is null during t_{on} . From these considerations it is possible to obtain the equivalent circuit sketched in figure 11 where there is a supply voltage $V_s D$ at the input terminals which is series connected to a voltage dependent voltage source equal to $V_o(1-D)$. A current dependent current source supplies the load and the capacitor C .

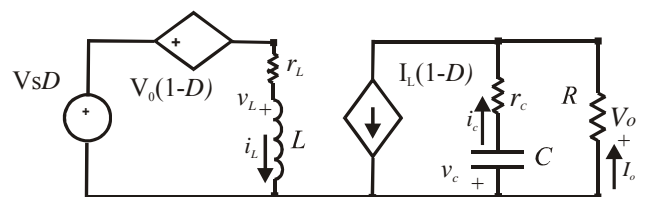


Fig. 11. Equivalent circuit of the buck-boost converter

The state space equations can be derived by the circuit of figure 11 using the LKV applied to the input loop and the LKI to the output node. These equations are the same

obtained for the boost converter in which there is $V_s D$ in place of V_s . The state space equations are given by.

$$\begin{cases} \frac{di_L}{dt} = -\frac{i_L r_L}{L} - \frac{v_c}{L}(1-D) + \frac{DV_s}{L} \\ \frac{dv_c}{dt} = \frac{i_L(1-D)}{C} - \frac{v_c}{RC} \end{cases} \quad (24)$$

A. Static Gain evaluation

The static gain can be obtained considering the circuit of figure 12, it is the DC version of the circuit of figure 11.

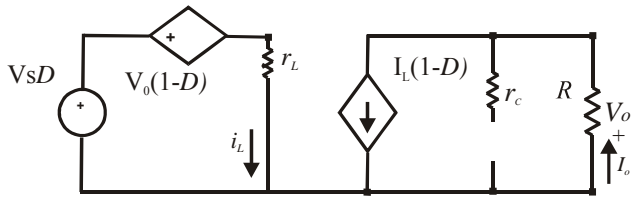


Fig. 12. Equivalent DC circuit of the buck-boost converter

The output voltage is given by the LKV applied to the input loop and the LKI to the output node:

$$V_0 = I_L(1-D)R = \frac{V_s D - V_0(1-D)}{r_L}(1-D)R \quad (25)$$

From (25) the static gain can be obtained.

$$\frac{V_0}{V_s} = \frac{RD(1-D)}{R(1-D)^2 + r_L} \quad (26)$$

It can be noted that (26) differs from (13) for the presence of $V_s D$ in place of V_s .

B. Audio susceptibility function

From the above considerations, the audio susceptibility function can be obtained substituting $V_s D$ in place of V_s , in (16).

$$\frac{\tilde{v}_0(s)}{\tilde{v}_s(s)} = \frac{(sCr_c + 1)RD(1-D)}{s^2RLC + s[L + RCr_L + (1-D)^2RCr_c] + R(1-D)^2 + r_L} \quad (27)$$

C. Control-to-output transfer function

The control to output transfer function can be calculated by the LKI on the output node. It differs from (16) for the presence of $V_s D$ in place of V_s . Taking into account (17) and neglecting the products of AC terms the following equation is obtained:

$$\frac{\tilde{v}_0(s)}{\tilde{d}(s)} = \frac{[-V_s(1-2D) + 2V_0(1-D)](sCr_c + 1)R}{s^2RLC + s[L + RCr_L + (1-D)^2RCr_c] + R(1-D)^2 + r_L} \quad (28)$$

D. Output impedance

The output impedance of the buck-boost converter can be calculated by the circuit drawn in figure 13, it is obtained by the circuit of figure 11 where the supply V_s is set to zero. It can be observed that this circuit is the same of the circuit drawn in figure 9 for the boost converter. From this the same expression of the output impedance is obtained.

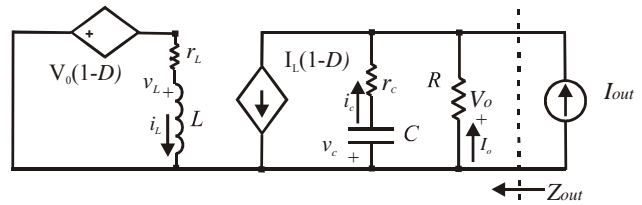


Fig. 13. Equivalent circuit of the buck-boost converter for calculating Z_{out} .

$$\begin{aligned} Z_{out} &= -\frac{\tilde{I}_{out}(s)}{\tilde{v}_0(s)} = \\ &= \frac{R(sCr_c + 1)(sL + r_L)}{s^2LC(R + r_c) + s[L + RCr_c(1-D)^2 + Cr_c(R + r_c)] + R(1-D)^2 + r_L} \end{aligned} \quad (29)$$

6. Simulink® implementation of the buck converter

Firstly, it is convenient to consider the implementation of the output capacitor and the load R which are parallel connected. Their impedance is given by:

$$Z_C // R = \frac{R\left(\frac{1}{sC} + r_c\right)}{R + r_c + \frac{1}{sC}} \cong R \frac{1 + sCr_c}{1 + sCR} \quad (30)$$

Alternatively eq. (30) can be written as:

$$Z_C // R \approx \frac{r_c + \frac{1}{sC}}{1 + \frac{1}{sCR}} = R \frac{\frac{1}{sCR}}{1 + \frac{1}{sCR}} + r_c \frac{1}{1 + \frac{1}{sCR}} \quad (31)$$

It suggests an implementation as a feedback system as shown in figure 14.

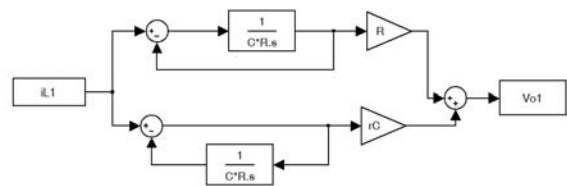


Fig. 14. Equivalent representation of the parallel connection of the load R and the capacitor C including its parasitic resistance.

It can be noted that the load resistor R appears as a coefficient in the transfer function; alternatively it can be implemented to be treated as an input parameter as shown in figure 15a. This scheme can be considered as a subsystem having the inductor current and the load resistance as inputs and the load voltage as output (see figure 15b). It can be noted that in this case only integrators are employed.

The mean node voltage method allows DC/DC converters to be easily implemented in Simulink® environment. As a matter of fact, the output voltage of the buck converter V_o is given by the inductor current flowing through the impedance ($Z_C // R$). This current is obtained as the

difference between $V_s D$ and V_o divided by the impedance of the inductance.

The buck converter is shown in figure 16. The value of the duty cycle is given as input to the PWM modulator, it gives the square wave that drives the power device. The load is given by the resistance R ; anyway a current representing the current required as example by an inverter can be added by a sum block at the inductor output.

7. Simulink® implementation of the boost converter

The boost converter scheme implemented in Simulink® environment is shown in figure 16.

It is based on the equivalent circuit of figure 8 in which the current of the inductance is obtained as the difference between V_s and $V_o(1-D)$; then this current is taken as the input of the parallel connection of the capacitor and the load represented as a subsystem.

8. Simulink® implementation of the buck-boost converter

The buck-boost converter scheme is shown in figure 17. It can be obtained from the same considerations made for the boost where the input voltage V_s is multiplied by the duty cycle D .

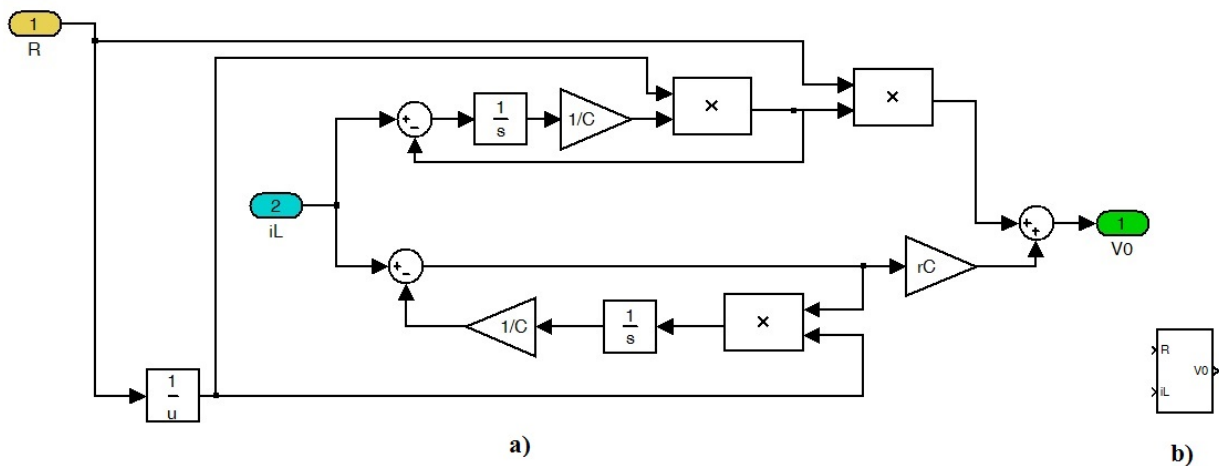


Fig. 15. Equivalent scheme of the parallel connection of the load and the capacitor in which the load is considered as an input parameter (a), and its representation as a subsystem (b).

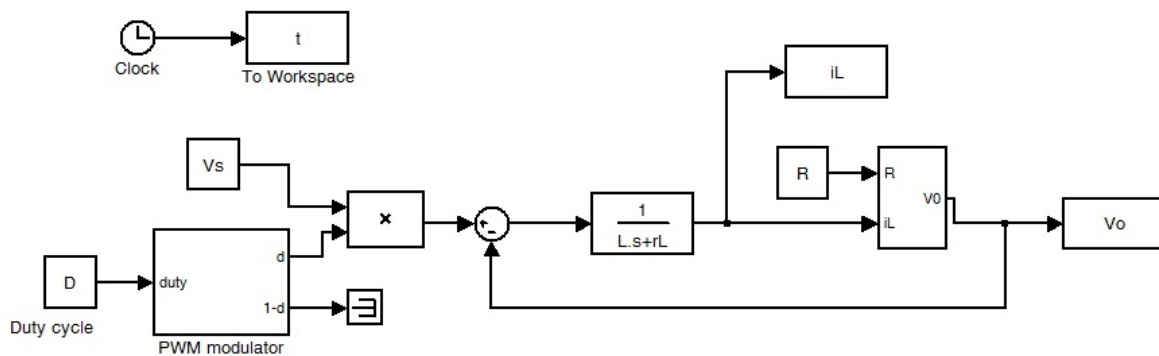


Fig. 16. Simulink® scheme of the buck converter.

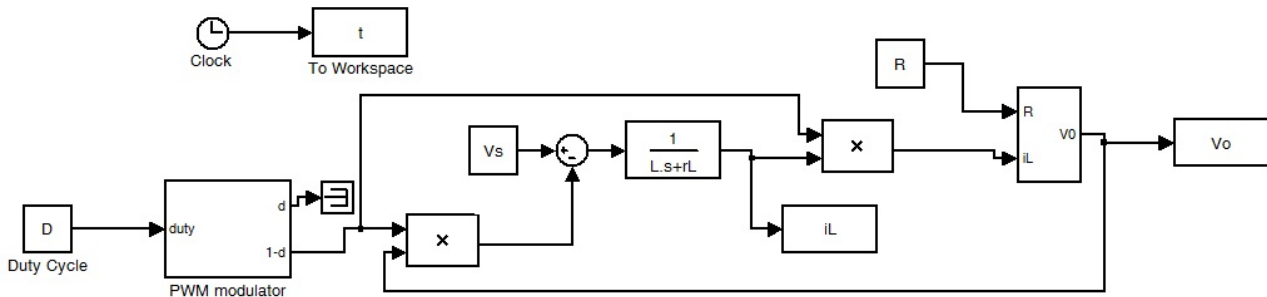


Fig. 17. Simulink® scheme of the boost converter.

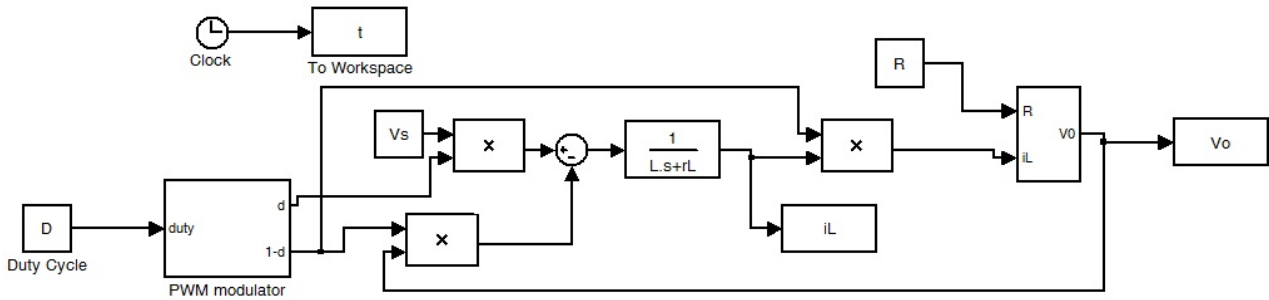


Fig. 18. Simulink® scheme of the buck-boost converter.

9. Simulation of a Buck converter

A buck converter has been simulated according to the scheme of figure 16. The parameters of the circuit are given in table I.

Table I: parameters of the buck converter

Component	symbol	value
Power IGBT		SGP04N60
Power diode		MURB820
inductance	L	100 μH
Parasitic resistance of L	r _L	0.3 Ω
Output Capacitor	C	33 μF
Parasitic resistance of C	r _C	0.2 Ω
Input voltage	V _s	12 V
Output voltage	V _o	5 V
Load	R	5 Ω
Switching frequency	f _s =1/T _s	20 kHz

The converter is operated in open-loop mode and the duty cycle has been set to obtain an output voltage equal to 5V. The voltage drop of the IGBT with its internal resistance and the voltage drop of the diode have been accounted for; the duty cycle calculated by (6) is equal to 0.48 and the corresponding expected voltage ripple of the output voltage is given by:

$$\Delta V_o = V_o \frac{1(1-D)}{8 f_s^2 LC} = 0.25 V \quad (32)$$

The boundary current, the critical inductance L_C and the current ripple on the inductor are given respectively by:

$$I_B = [V_o(1-D)]/2f_s L_C = 1 A \quad (33)$$

$$L_C = [R(1-D)]/2f_s = 65 \mu H \quad (34)$$

$$\Delta I_L = [(V_s - V_o)T_{on}]/L = 1.44 A \quad (35)$$

On this basis a continuous operating mode is expected. The waveforms obtained by the scheme of figure 16 are sketched in figure 19. It can be noted that the mean value of the current flowing through the inductor corresponds to the load current and the converter operates in continuous mode as expected. Finally the voltage ripple on the load is higher than the value calculated by (32) since it is influenced by the relatively high value of the parasitic

resistance of the output capacitor, it implies that its shape is different from a sinusoidal one.

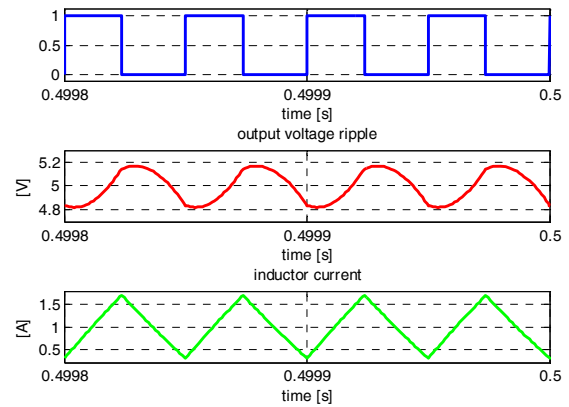


Fig. 19. Duty cycle (top), output voltage ripple (middle) and inductor current (bottom) obtained by simulation.

10. Experimental Results

A prototype of the converter has been built with the components of table I and the waveforms have been measured by an Agilent MSO6104A 1 GHz oscilloscope, a 50 MHz current probe Agilent 1147 and a voltage probe 10073C. The corresponding waveforms are given in figure 20.

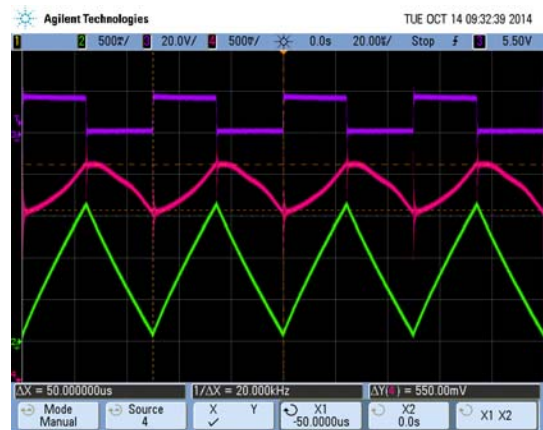


Fig. 20. Duty cycle (top), output voltage ripple (middle) and inductor current (bottom) obtained by experiment.

It can be noted that the measured values correspond to those obtained in simulation. In particular, the output voltage ripple has the same shape of the simulated waveform and a peak-to-peak amplitude higher of about

10%. It is influenced by commutation spikes that are not modelled. The inductor current exhibits a peak-to-peak value of about 1.6 A. These results confirm the goodness of the proposed model. Finally the calculation time has been compared with an implementations in the same Simulink® environment, using the Power System Blockset where the real power switches models are used. Results have shown that the simulation with real power switches requires a time higher of about 127% compared to the proposed method.

11. Conclusions

An analysis of buck, boost and buck-boost converters by the mean node voltage method has been proposed. The proposed approach has the following advantages: a) it allows the characteristic functions of a DC/DC converter to be easier calculated compared to the state space state averaging method; b) it does not require a specific circuit simulator taking into account the parasitic effects of inductors, capacitors and power switches; c) it has a faster of computation time, compared to an implementation in which real switches are used. In addition the implementation is devised to avoid the implementation of derivative blocks. The characteristic waveforms obtained by simulation for a buck converter have been compared to experimental ones showing a good agreement.

The proposed approach can be followed for the analysis of more complicated DC/DC converter topologies. On the other hand, this implementation does not take into account high frequency effects due to the power devices behaviour however they can be evaluated by adopting a dedicated high frequency model of the power devices.

Acknowledgement

This paper has been funded by the research project: RITmare, Ricerca Italiana per il mare (Italian Research for the sea) CUP:B91J11000740001.

The author is grateful to Mr. Antonio Sauro and Mr. Giuseppe Santo Scordato, technicians at the ISSIA-CNR, for the irreplaceable contribution in building the DC/DC converter and the set-up of the measurement system.

References

[1] S. Ang, A. Oliva, Power Switching Converters, CRC Press, Taylor and Francis Group, Boca Raton, FL 2011.
 [2] H. Sira-Ramirez, R. Silva-Ortigoza, Control Design Technique in Power Electronics Devices, Springer Verlag, London 2006.
 [3] K. Wu, Switch-Mode Power Converters, Academic Press, London 2009.
 [4] Di Piazza, M. C., Vitale G., Photovoltaic Sources: Modelling and Emulation, Springer, 2013.
 [5] R. Teodorescu, M. Liserre, P. Rodriguez, "Grid Converters for Photovoltaic and Wind Power Systems", Wiley, 2011.
 [6] F. Blaabjerg, K. Ma, D. Zhou, "Power electronics and reliability in renewable energy systems", 2012 IEEE International Symposium on Industrial Electronics (ISIE), Hangzhou, China, May 28-31, 2012.
 [7] F. Blaabjerg, M. Liserre, K. Ma, "Power Electronics Converters for Wind Turbine Systems, IEEE Trans on Industry Applications, vol. 48, n. 2, March/April 2012
 [8] F. Blaabjerg, F. Iov, T. Kerekes, R. Teodorescu, "Trends in power electronics and control of renewable energy systems". 14th International Power Electronics and Motion Control

Conference (EPE/PEMC), Ohrid (Republic of Macedonia) September 6-8, 2010.

[9] G. Graditi, S. Favuzza, F. Spertino, G. Vitale, "Comparison of Power Quality Impact of Different Photovoltaic Inverters: the viewpoint of the grid", IEEE International Conference on Industrial Technology, ICIT-2004, 8-10 Dec. 2004.
 [10] M. C. Di Piazza, M. Pucci, A. Ragusa, G. Vitale "Fuzzified PI Voltage Control for Boost Converters in Multi-String PV Plants", 34th Annual Conference of the IEEE Industrial Electronics Society, IECON-2008. 10-13 November 2008
 [11] M. C. Di Piazza, G. Vitale "Efficiency Comparison of Grid Side Converters for DC Distribution Systems", International Conference on Renewable Energy and Power Quality (ICREPQ'13), Special session on Power Electronics for Renewable Energy Systems, Bilbao (Spain), 20-22 of March 2013.
 [12] M. Saedifard, M. Graovac, R.F. Dias, R. Iravani, "DC Power Systems: Challenges and Opportunities", IEEE Power and Energy society meeting, Minneapolis, 25-29 July 2010.
 [13] H. Kakigano, N. Nomura, T. Ise, "Loss evaluation of DC distribution for residential houses compared with AC system", in Proc. 2010 International Power Electronics Conference (IPEC), 2010, pp 480-486.
 [14] M. Cirrincione, M. Cossentino, S. Gaglio, V. Hilaire, A. Koukam, M. Pucci, L. Sabatucci, G. Vitale, "Intelligent Energy Management System", 7th IEEE International Conference on Industrial Informatics INDIN 2009, 24-26th June 2009, Cardiff, UK.
 [15] M. Rodriguez, G. Stahl, L. Corradini, D. Maksimović, "Smart DC Power Management System Based on Software-Configurable Power Modules", IEEE Trans. on Power Electronics, vol. 28, no. 4, april 2014.
 [16] P. Chiang Loh, D. Li, Yi Kang Chai, F. Blaabjerg, "Autonomous Operation of Hybrid Microgrid With AC and DC Subgrids", IEEE trans. On Power Electronics, vol 28, n. 5, May 2013.
 [17] A. Ragusa, M. C. Di Piazza, M. Pucci, G. Vitale, "Analytical versus Neural Real-time Simulation of a Photovoltaic Generator based on a DC-DC Converter", IEEE Transactions on Industry Applications vol. 46, no. 6, nov/dec 2010. pp. 2501-2510
 [18] M.C. Di Piazza, G. Vitale, "Photovoltaic field emulation including dynamic and partial shadow conditions", Applied Energy, n. 87 (2010) pp. 814–823.
 [19] G. Marsala, M. Pucci, G. Vitale, M. Cirrincione, A. Miraoui, "A Prototype of a Fuel Cell PEM Emulator Based on a Buck Converter", Applied Energy, vol. 86, issue 10, pp.2192-2203, Oct 2009.
 [20] M. Cirrincione, M. C. Di Piazza, G. Marsala, M. Pucci, G. Vitale, "Real Time Simulation of Renewable Sources by Model-Based Control of DC/DC Converters", IEEE International symposium on Industrial Electronics, ISIE 08, 29 June 2 July 2008 Cambridge (UK).
 [21] R. W. Erickson, D. Maksimovic: "Fundamentals of Power Electronics", Kluwer Academic Publishers, New York 2004.